

An implementation of the microphysics in full general relativity : General relativistic neutrino leakage scheme

Yuichiro Sekiguchi

Division of Theoretical Astronomy, National Astronomical Observatory of Japan,
Mitaka, Tokyo 181-8588, Japan

E-mail: sekig@th.nao.ac.jp

Abstract.

Performing fully general relativistic simulations taking account of microphysical processes (e.g., weak interactions and neutrino cooling) is one of long standing problems in numerical relativity. One of main difficulties in implementation of weak interactions in the general relativistic framework lies on the fact that the characteristic timescale of weak interaction processes (the WP timescale, $t_{\text{wp}} \sim |Y_e/\dot{Y}_e|$) in hot dense matters is much shorter than the dynamical timescale (t_{dyn}). Numerically this means that *stiff* source terms appears in the equations so that an implicit scheme is in general necessary to stably solve the relevant equations. Otherwise a very short timestep ($\Delta t < t_{\text{wp}} \ll t_{\text{dyn}}$) will be required to solve them explicitly, which is unrealistic in the present computational resources. Furthermore, in the relativistic framework, the Lorentz factor is coupled with the rest mass density and the energy density. The specific enthalpy is also coupled with the momentum. Due to these couplings, it is very complicated to recover the primitive variables and the Lorentz factor from conserved quantities. Consequently, it is very difficult to solve the equations implicitly in the fully general relativistic framework. At the current status, no implicit procedure have been proposed except for the case of the spherical symmetry. Therefore, an approximate, explicit procedure is developed in the fully general relativistic framework in this paper as an first implementation of the microphysics toward a more realistic sophisticated model. The procedure is based on the so-called neutrino leakage schemes which is based on the property that the characteristic timescale in which neutrinos leak out of the system (the leakage timescale, t_{leak}) is much longer than the WP timescale. In the previous leakage schemes, however, the problems of the stiff source terms are avoided in an artificial manner. In this paper, I present a detailed neutrino leakage scheme and a simple and stable method for solving the equations explicitly in the fully general relativistic framework. The drawback of the artificial treatment of the stiff source terms is improved. I also perform a test simulation to check the validity of the present method, showing that it works fairly well.

1. Introduction

1.1. Motivation

Numerical relativity is the unique and powerful tool to explore dynamical phenomena in which strong gravity plays important roles. Stellar core collapse and mergers of compact star binaries are among the most important and interesting events in the field. In theoretical view points, performing simulations of these phenomena is one of challenging problems because a rich diversity of physics has to be taken into account. All four known forces of nature are involved and play important roles during the collapse. General relativistic gravity plays essential roles in formation of a black hole. Note also that general relativity may play important roles in supernova explosion as previous pioneering works [1, 2] showed. The weak interactions and emission of neutrinos govern energy and lepton-number losses, and hence driving the thermal and chemical evolutions of the system. The strong interactions determine ingredients and properties of dense matters. Strong magnetic fields, if they are present, may modify the dynamics.

There is a long list of studies which explore these phenomena in the framework of numerical relativity (see [3] and references therein for recent simulations of stellar core collapse, and see [4, 5] and references therein for those of compact binary merger). In most of the previous studies, however, treatments of microphysics are very simplified and more sophisticated studies are necessary.

Furthermore, recent observations [6, 7, 8, 9, 10, 11, 12] have discovered the spectroscopic connections between several supernovae and long gamma-ray bursts (GRBs), clarifying that at least some of long GRBs are associated with the collapse of massive stars. Also, there are theoretical models that a short GRB occurs as a result of a binary neutron star merger [13, 14]. The relevant process of the energy deposition to form a GRB fireball may be pair annihilation of neutrinos emitted from a hot massive disk around a black hole formed after the collapse or the merger. These also enhance the importance of exploring stellar core collapse and coalescence of compact star binary in full general relativity taking account of microphysical processes.

Gravitational wave astronomy will start in this decade. The first generation of ground-based interferometric detectors (LIGO [15], VIRGO [16], GEO600 [17]) are now in the scientific search for gravitational waves. To obtain physically valuable information from these observations, it is necessary to connect the observed data and the physics behind it. For this purpose, performing numerical simulation is the unique approach. However, accurate predictions of gravitational waveforms are still hampered by the facts that reliable estimates of waveforms require a general relativistic treatment [18, 19], and that appropriate treatments of microphysics such as a nuclear equation of state (EOS), the electron capture, and neutrino emissions and transfers. General relativistic simulations including microphysics are required to make accurate predictions of gravitational waveforms.

As described above, to perform multidimensional simulations in the frame work of numerical relativity implementing microphysics is currently one of the most important

subjects in theoretical astrophysics. In spherical symmetry, fully general relativistic simulations [20, 21, 22] of stellar core collapse have been performed in so-called state-of-the-art manners, namely, employing realistic equations of state, taking account of relevant microphysics, and solving the Boltzmann equation for the transfer of neutrinos (see also [23]). In the multidimensional case, by contrast, there are few studies in the framework of general relativity. Recently, general relativistic simulations implementing a realistic EOS and the electron capture were performed [24, 25]. In their calculation, however, the electron capture rate is not calculated in a self-consistent manner. Instead, they adopted a simplified prescription proposed in [26], which is based on results of spherically symmetric simulations. It is not clear whether this treatment is justified for non-spherical collapse and the multidimensional phenomena. More importantly, they did not take account of neutrino cooling.

Recently, I have made a fully general relativistic code with microphysics for the first time [27]. Since it is currently impossible to fully solve the multidimensional neutrino transfer equations in the framework of full general relativity because of restrictions of computational resources, it will be reasonable to adopt an approximated treatment of neutrino cooling. In that work, a general relativistic version of the so-called neutrino leakage schemes is developed.

1.2. Neutrino leakage scheme

The leakage schemes [28, 29, 30, 31, 32] as an approximate method for the neutrino cooling has a well-established history (e.g. [31]). The basic concept of the original neutrino leakage schemes [28, 29] is to treat the following two regions in the system separately: one region is where the diffusion timescale of neutrinos is longer than the dynamical timescale, and hence neutrinos are 'trapped' (neutrino-trapped region); the other region is where the diffusion timescale is shorter than the dynamical timescale, and hence neutrinos stream out freely out of the system (free-streaming region). The idea of treating the diffusion region separately has been applied to more advanced methods for the neutrino transfer (see e.g., [33] and references therein).

Then, electron neutrinos and anti-neutrinos in the neutrino-trapped region are assumed to be in β -equilibrium state. The *net* local rates of lepton-number and energy exchange with matters are set to be zero in the neutrino-trapped region. To treat diffusive 'leakage' of neutrinos out of the neutrino-trapped region, phenomenological source terms based on the diffusion theory are introduced [28, 29]. In the free-streaming region, on the other hand, it is assumed that neutrinos escape from the system without interacting with matter. Therefore, neutrinos carry the lepton number and the energy according to the local weak interaction rates. The neutrino fractions are not solved in the original version of the leakage scheme: Only the total lepton fraction is necessary in the free-streaming region and the neutrino fractions are set to zero in the free-streaming region. Note that there is a sharp discontinuity between the two regions. Consequently, thermodynamical quantities, in particular those of neutrinos and the electron fraction,

are also discontinuous at the boundary.

The *transfer* of neutrinos are not solved in the leakage schemes. Therefore, they cannot treat *non-local* interactions among the neutrinos and matters; for example, the so-called neutrino heating [34] and the neutrino pair annihilation cannot be treated in the leakage scheme. Nevertheless, I consider a detailed general relativistic leakage scheme presented in this paper to be an important step towards more reliable and sophisticated models, since the simulated physical timescales in the case of compact binary mergers will be order of 10 ms and neutrino transfer is expected to be unimportant [35], and since the neutrino heating would be not very important in the case of prompt black hole formation.

Usually, the boundary between the neutrino-trapped and free-streaming regions is given by hand as a single 'neutrino-trapping' density (ρ_{trap}) in the previous simulations of stellar core collapse [28, 29, 32]. In fact, however, the location at which the neutrino trapping occurs depends strongly on the neutrino energies (ϵ_ν), and hence, there are different neutrino-trapping densities for different neutrino energies. The neutrino-trapping densities depend strongly on the neutrino energies as $\rho_{\text{trap}} \propto \epsilon_\nu^{-3}$ [36]. This implies that neutrinos with lowest energy leave their corresponding neutrino-trapping region first, and neutrinos with higher energy are emitted later.

In the previous leakage schemes [28, 29, 32], on the other hand, all neutrinos are emitted in one moment irrespective of their energy. Consequently in the case of the so-called neutrino burst emission (e.g., [36]), for example, the duration in which the neutrinos are emitted is shortened and the peak luminosity at the burst is overestimated in the previous leakage schemes [29, 27]. The dependence of the neutrino-trapping densities and neutrino diffusion rates on the neutrino energies are approximately taken into account in the recent simulations of binary neutron star mergers [37, 35]. However the lepton-number conservation equations for neutrinos are not solved [37].

Recently, a numerical code based on a relativistic extension of the leakage schemes was developed in [27], where not the region of the system but the energy momentum tensor of neutrinos are decomposed into two parts; 'trapped-neutrino' and 'streaming-neutrino' parts. However the source terms of hydrodynamic and the lepton-number-conservation equations are determined using the single neutrino-trapping density as in the case of the previous leakage schemes. More recently, Liebendörfer et al. [38] proposed a scheme, which they call the isotropic diffusion source approximation, where the neutrino distribution function is decomposed into an isotropic distribution function of trapped neutrinos and a distribution function of streaming neutrinos.

The present work is based on the previous studies described above. The framework of general relativistic extension of leakage scheme is based on my previous study in [27]. The treatment of neutrino diffusion rates is based on the recent work by Rosswog and Liebendörfer [35] where the neutrino-energy dependences are taken into account. Thus the remaining main problem to implement the relevant microphysics is that straightforward explicit scheme cannot be adopted to solve the equations [40] since the characteristic timescale of weak interaction processes ($t_{\text{wp}} \sim |Y_e/\dot{Y}_e|$, hereafter the

WP timescale) is much shorter than the dynamical timescale (t_{dyn}) in hot dense regions, as described in Sec. 2. Note that the WP timescale is different from the so-called weak timescale. In this paper I present a simple and stable method in which the equations are solved explicitly in the *dynamical timescale* in the fully general relativistic framework.

The paper is organized as follows. First, main difficulties of implementation of weak interactions and neutrino cooling in full general relativity compared to implementation of them in Newtonian framework are briefly summarized in Sec. 2. Then, framework of the implementation of the microphysics is described in detail in Sec. 3. Some details of microphysics and numerics are described in Sec. 4, although GR leakage framework is independent of specific implementations of microphysics. In Sec. 5, results of a test simulation is briefly described illustrating good ability of the present implementation. Section 6 is devoted to the summary and discussions. Throughout the paper, the geometrical unit $c = G = 1$ is used otherwise stated.

2. Difficulties of implementation of weak interactions and neutrino cooling in full general relativity

Since the characteristic timescale of weak interaction precesses (the WP timescale $t_{\text{wp}} \sim |Y_e/\dot{Y}_e|$) is much shorter than the dynamical timescale t_{dyn} in hot dense matters [40, 35], the numerical treatment of the weak interactions cannot be explicit, as noted in the previous pioneering work by Bruenn [40]. Otherwise a very short timestep ($\Delta t < t_{\text{wp}} \ll t_{\text{dyn}}$) will be required to solve the equations explicitly, which is unrealistic in the present computational resources.

The *net* rates of lepton-number and energy exchanges between matters and neutrinos may not be large, and consequently an *effective* timescale apparently may not be short compared to the dynamical timescale. However, this does not immediately imply that one can solve the equations explicitly without bringing in any devices. For example the net electron capture rate vanishes in the β -equilibrium. The achievement of β -equilibrium is consequences of both cancellation of two very *large* weak interaction processes (the electron and the electron-neutrino captures) and the action of the phase space blocking. Note that the weak interaction processes depend enormously on the temperature and the lepton chemical potentials. Therefore, small error in evaluations of the temperature and a small deviation from the β -equilibrium due to small error in estimation of the lepton fractions will produce large error and stiff source terms, and consequently the explicit numerical evolutions may become unstable.

In the following of this section, I describe difficulties of implementation of weak interactions and neutrino cooling into the hydrodynamic equations in the conservative schemes in full general relativity *compared with the Newtonian framework*.

In the Newtonian framework, the equations may be solved implicitly [39, 40, 41, 42, 43, 44, 45, 46, 47] (see also [48, 33] and references therein). The equations of hydrodynamics, lepton-number conservations, and neutrino processes are schematically

written as,

$$\dot{\rho} = 0, \quad (1)$$

$$\dot{v}_i = S_{v_i}(\rho, Y_e, T, Q_\nu), \quad (2)$$

$$\dot{Y}_e = S_{Y_e}(\rho, Y_e, T, Q_\nu), \quad (3)$$

$$\dot{e} = S_e(\rho, Y_e, T, Q_\nu), \quad (4)$$

$$\dot{Q}_\nu = S_{Q_\nu}(\rho, Y_e, T, Q_\nu), \quad (5)$$

where ρ is the rest mass density, v_i is the velocity, Y_e is the electron fraction, e is the (internal) energy of matter, T is the temperature and Q_ν stands for the relevant neutrino quantities. S 's in the right hand side stand for the relevant source terms. Comparing the quantities in the left-hand-side and the argument quantities in the source terms, only the relation between e and T is nontrivial. Usually, EOSs employed in the simulation is tabularized, and one dimensional search over the EOS table is required to solve them. To achieve this procedure in an implicit manner is quite a difficult problem.

In the relativistic framework, the situation becomes much more complicated in conservative schemes, since the Lorentz factor (Γ) is coupled with rest mass density and the energy density (see Eqs. (40) and (47)), and since the specific enthalpy ($h = h(\rho, Y_e, T)$) is coupled with the momentum (see Eq. (45)).

It should be addressed that the previous fully general relativistic works in the spherical symmetry [20, 21] are based on the so-called Misner-Sharp coordinates [49]. There are no such complicated couplings in this Lagrangian coordinates. Accordingly the equations may be solved essentially in the same manner as in the Newtonian framework. In multidimensional case, on the other hand, no Lagrangian coordinates are known, and the Eulerian coordinates are adopted. In the Eulerian coordinate, the complicated couplings inevitably appear in multidimensional case.

Omitting the factors associated with the geometric variables (which are known when solving hydrodynamics equations), the equations to be solved in the relativistic framework are schematically written as,

$$\dot{\rho}_*(\rho, \Gamma) = 0, \quad (6)$$

$$\dot{\hat{u}}_i(u_i, h) = \dot{\hat{u}}_i(u_i, \rho, Y_e, T) = S_{\hat{u}_i}(\rho, Y_e, T, Q_\nu, \Gamma), \quad (7)$$

$$\dot{Y}_e = S_{Y_e}(\rho, Y_e, T, Q_\nu, \Gamma), \quad (8)$$

$$\dot{\hat{e}}(\rho, Y_e, T, \Gamma) = S_{\hat{e}}(\rho, Y_e, T, Q_\nu, \Gamma), \quad (9)$$

$$\dot{Q}_\nu = S_{Q_\nu}(\rho, Y_e, T, Q_\nu, \Gamma), \quad (10)$$

where ρ_* is a weighted density, \hat{u}_α is a weighted four velocity, \hat{e} is a weighted energy density (see Sec. 3.4 for the definition of these variables). Note that the Lorentz factor is appeared in the equations.

The Lorentz factor is calculated by solving the normalization condition $u^\alpha u_\alpha = -1$, which is rather complicated nonlinear equation schematically written as

$$f_{\text{normalization}}(\hat{u}_i, \Gamma) = f_{\text{normalization}}(u_i, \rho, Y_e, T, \Gamma) = 0. \quad (11)$$

(For a solution of the equation in practice, see Sec. 3.5.) The accurate calculation of the Lorentz factor and the accurate solution of the normalization condition are very important in the numerical relativistic hydrodynamics.

Now, it is obvious that the argument quantities in the source terms are not simply related with the left-hand-side evolved quantities in Eqs. (6)–(11). To solve the equations implicitly is quite difficult and there are even no successful formulations. Moreover it is not clear whether a convergent solution can be *stably* obtained numerically or not, since they are simultaneous nonlinear equations. Therefore, it may not be a poor choice to adopt an alternative approach in which the equations are solved explicitly with some approximations (see Sec. 3).

The second minor problem which is not exist in the Newtonian framework is that one cannot add any microphysical processes in forms of 'cooling' or 'heating' terms Q_α , into the right hand side of hydrodynamic equations as

$$\nabla_\alpha T_\beta^\beta = Q_\beta. \quad (12)$$

Instead, the energy-momentum tensor of neutrinos should be introduced in the general relativistic framework:

$$(T^{\text{tot}})_{\alpha\beta} = (T^{\text{F}})_{\alpha\beta} + (T^\nu)_{\alpha\beta}, \quad (13)$$

where T^{tot} , T^{F} , and T^ν are the total energy-momentum tensor and energy-momentum tensor of fluid and neutrino parts, respectively (see Sec. 3 for the definition). Now, one should solve the following coupled equations

$$\nabla_\alpha (T^{\text{F}})^\alpha_\beta = Q_\beta, \quad (14)$$

$$\nabla_\alpha (T^\nu)^\alpha_\beta = -Q_\beta. \quad (15)$$

Here, the source term Q_α can be regarded as the local production of neutrinos through the weak processes, ignoring non-local neutrino capture on matter.

3. General relativistic neutrino leakage scheme

In the following, I describe in some detail a method for solving all of the equation in an explicit manner. As described in the previous section, since $t_{\text{wp}} \ll t_{\text{dyn}}$ in the hot dense matter regions, the source terms in the equations become too *stiff* to be solved explicitly. The characteristic timescale of leakage of neutrinos from the system t_{leak} , however, is much longer than t_{wp} in the hot dense matter region. Note that $t_{\text{leak}} \sim L/c \sim t_{\text{dyn}}$ where L is the characteristic length scale of the system. On the other hand, t_{leak} is comparable to t_{wp} in the free-streaming regions where the WP timescale is longer than or comparable with the dynamical timescale. Utilizing these facts, I approximate the original matter equations and reformulate them so that the source terms are to be characterized by the leakage timescale t_{leak} .

3.1. Decomposition of neutrino energy-momentum tensor

Now, the problem is that the source term Q_α in Eqs. (14) and (15) becomes too *stiff* to solve explicitly in hot dense matter regions where $t_{\text{wp}} \ll t_{\text{dyn}}$. To overcome the situation, the following procedures are adopted.

First, it is assumed that the energy-momentum tensor of neutrinos are be decomposed into 'trapped-neutrino' $((T^{\nu,\text{T}})_{\alpha\beta})$ and 'streaming-neutrino' $((T^{\nu,\text{S}})_{\alpha\beta})$ parts as [27],

$$(T^\nu)_{\alpha\beta} = (T^{\nu,\text{T}})_{\alpha\beta} + (T^{\nu,\text{S}})_{\alpha\beta}. \quad (16)$$

Here, the trapped-neutrinos phenomenologically represent neutrinos which interact sufficiently frequently with matter and are thermalized, while the streaming-neutrino part describes a phenomenological flow of neutrinos streaming out of the system [27] (see also [38] where a more sophisticate method based on the distribution function is adopted in the Newtonian framework).

Second, the locally produced neutrinos are assumed to *leak out* to be the streaming-neutrinos with a leakage rate Q_α^{leak} :

$$\nabla_\beta (T^{\nu,\text{S}})_\alpha^\beta = Q_\alpha^{\text{leak}}. \quad (17)$$

Then, the equation of the trapped-neutrino part becomes

$$\nabla_\beta (T^{\nu,\text{T}})_\alpha^\beta = Q_\alpha - Q_\alpha^{\text{leak}}. \quad (18)$$

Third, the trapped-neutrino part is combined with the fluid part to give

$$T_{\alpha\beta} \equiv (T^{\text{F}})_{\alpha\beta} + (T^{\nu,\text{T}})_{\alpha\beta}, \quad (19)$$

and Eqs. (14) and (18) are combined to give

$$\nabla_\beta T_\alpha^\beta = -Q_\alpha^{\text{leak}}. \quad (20)$$

Thus the equations to be solved is changed from Eqs. (14) and (15) to Eqs. (20) and (17). Note that the new equations only include the source terms Q_α^{leak} which is characterized by the leakage timescale t_{leak} . Definition of Q_α^{leak} will be found in Sec. 3.3.

The energy-momentum tensor of the fluid and trapped-neutrino parts $(T_{\alpha\beta})$ is treated as that of the perfect fluid

$$T_{\alpha\beta} = (\rho + \rho\varepsilon + P)u_\alpha u_\beta + P g_{\alpha\beta}, \quad (21)$$

where ρ and u^α are the rest mass density and the 4-velocity. The specific internal energy density (ε) and the pressure (P) are the sum of the contributions from the baryons (free protons, free neutrons, α -particles, and heavy nuclei), leptons (electrons, positrons, and *trapped-neutrinos*), and the radiation as,

$$P = P_B + P_e + P_\nu + P_r, \quad (22)$$

$$\varepsilon = \varepsilon_B + \varepsilon_e + \varepsilon_\nu + \varepsilon_r, \quad (23)$$

where subscripts 'B', 'e', 'r', and ' ν ' denote the components of the baryons, electrons and positrons, radiation, and trapped-neutrinos, respectively.

The streaming-neutrino part, on the other hand, is set to be a general form of

$$(T^{\nu,S})_{\alpha\beta} = En_\alpha n_\beta + F_\alpha n_\beta + F_\beta n_\alpha + P_{\alpha\beta}, \quad (24)$$

where $F_\alpha n^\alpha = P_{\alpha\beta} n^\alpha = 0$. In order to close the system, we need an explicit expression of $P_{\alpha\beta}$. In this paper, I adopt a rather simple form $P_{\alpha\beta} = \chi E \gamma_{\alpha\beta}$ with $\chi = 1/3$. This approximation may work well in high density regions but will violate in low density regions. However, the violation will not affect the dynamics since the total amount of streaming-neutrinos emitted in low density regions will be small. Of course, a more sophisticated treatment will be necessary in a future study.

3.2. The lepton-number conservation equations

The conservation equations of the lepton fractions can be written schematically as

$$\frac{dY_e}{dt} = -\gamma_e, \quad (25)$$

$$\frac{dY_{\nu e}}{dt} = \gamma_{\nu e}, \quad (26)$$

$$\frac{dY_{\bar{\nu} e}}{dt} = \gamma_{\bar{\nu} e}, \quad (27)$$

$$\frac{dY_{\nu x}}{dt} = \gamma_{\nu x}, \quad (28)$$

where Y_e , $Y_{\nu e}$, $Y_{\bar{\nu} e}$, and $Y_{\nu x}$ denote the electron fraction, the electron neutrino fraction, the electron anti-neutrino fraction, and μ and τ neutrino and anti-neutrino fractions, respectively. It should be addressed that, in the previous simulations based on the leakage schemes [28, 29, 32, 37], the neutrino fractions are not solved.

The source terms of neutrino fractions can be written, on the basis of the present leakage scheme, as

$$\gamma_{\nu e} = \gamma_{\nu e}^{\text{local}} - \gamma_{\nu e}^{\text{leak}}, \quad (29)$$

$$\gamma_{\bar{\nu} e} = \gamma_{\bar{\nu} e}^{\text{local}} - \gamma_{\bar{\nu} e}^{\text{leak}}, \quad (30)$$

$$\gamma_{\nu x} = \gamma_{\nu x}^{\text{local}} - \gamma_{\nu x}^{\text{leak}}, \quad (31)$$

where $\gamma_\nu^{\text{local}}$ and γ_ν^{leak} are the local production and the leakage rates of neutrinos, respectively (see Sec. 3.3). Note that only the trapped-neutrinos are responsible for the neutrino fractions. The thermodynamical quantities (e.g., the pressure and the chemical potentials) of neutrinos can be calculated from the neutrino fractions on the assumption of thermalization of the trapped neutrinos.

The source term for the electron fraction conservation can be written

$$\gamma_e = \gamma_{\nu e}^{\text{local}} - \gamma_{\bar{\nu} e}^{\text{local}}. \quad (32)$$

Since $\gamma_\nu^{\text{local}}$ s are characterized by the WP timescale t_{wp} , some procedures are necessary to solve the lepton conservation equations explicitly. The following simple procedures are proposed to solve the equation stably.

First, in each timestep n , the conservation equation of the *total* lepton fraction ($Y_l = Y_e - Y_{\nu e} + Y_{\bar{\nu} e}$),

$$\frac{dY_l}{dt} = -\gamma_l, \quad (33)$$

is solved together with the conservation equation of $Y_{\nu x}$, Eq. (28), in advance of solving whole of the lepton conservation equations (Eqs. (25) – (28)). Note that the source term $\gamma_l = \gamma_{\nu e}^{\text{leak}} - \gamma_{\bar{\nu} e}^{\text{leak}}$ is characterized by the leakage timescale t_{leak} so that this equation may be solved explicitly in the hydrodynamic timescale. Then, assuming that the β -equilibrium is achieved, values of the lepton fractions in the β -equilibrium (Y_e^β , $Y_{\nu e}^\beta$, and $Y_{\bar{\nu} e}^\beta$) are calculated from evolved Y_l .

Second, regarding $Y_{\nu e}^\beta$ and $Y_{\bar{\nu} e}^\beta$ as the maximum allowed values of the neutrino fractions in the next timestep $n + 1$, the source terms are limited so that Y_ν 's in the timestep $n + 1$ do not exceed Y_ν^β 's. Then, the whole of the lepton conservation equations (Eqs. (25) – (28)) are solved explicitly utilizing the limiters.

Third, the following conditions are checked

$$\mu_p + \mu_e < \mu_n + \mu_{\nu e}, \quad (34)$$

$$\mu_n - \mu_e < \mu_p + \mu_{\bar{\nu} e}, \quad (35)$$

where μ_p , μ_n , μ_e , $\mu_{\nu e}$ and $\mu_{\bar{\nu} e}$ are the chemical potentials of protons, neutrons, electrons, electron neutrinos, and electron anti-neutrinos, respectively. If both conditions are satisfied, the values of the lepton fractions in the timestep $n + 1$ is set to be those in the β -equilibrium value; Y_e^β , $Y_{\nu e}^\beta$, and $Y_{\bar{\nu} e}^\beta$. On the other hand, if either or both conditions are not satisfied, the lepton fractions in the timestep $n + 1$ is set to be those obtained by solving whole of the lepton-number conservation equations.

A limiter for the evolution of $Y_{\nu x}$ may be also necessary in some case where the pair processes are dominant, for example, in simulations of collapse of population III stellar core. In this case, the value of $Y_{\nu x}$ at the pair equilibrium (i.e. at $\mu_{\nu x} = 0$), $Y_{\nu x}^{\text{pair}}$ may be used to limit the source term.

In the present implementation it is not necessary to somewhat artificially divide the system into neutrino-trapped and free-streaming regions. Therefore there is no discontinuous boundary which existed in the previous leakage schemes [28, 29, 32].

I found that simulations of the collapse of population III stellar core and the formation of a black hole, in which very high temperatures ($T > 100$ MeV) are achieved, can be stably performed using the simple procedure presented in this paper.

3.3. Definition of leakage rates

In this subsection the definitions of the leakage rates Q_α^{leak} and γ_ν^{leak} are presented. Because Q_ν^{leak} may be regarded as the emissivity of neutrinos measured in the *fluid rest frame*, Q_α^{leak} is defined as [50]

$$Q_\alpha^{\text{leak}} = Q_\nu^{\text{leak}} u_\alpha. \quad (36)$$

Note that although there may be a freedom to include terms H_α which satisfies $H_\alpha u^\alpha = 0$, Eq. (3.3) may be the best choice in the present framework.

The leakage rates Q_ν^{leak} and γ_ν^{leak} are assumed to satisfy the following properties.

- (i) The leakage rates approach the local rates Q_ν^{local} and $\gamma_\nu^{\text{local}}$ in the low density, transparent region.
- (ii) The leakage rates approach the diffusion rates Q_ν^{diff} and γ_ν^{diff} in the high density, opaque region.
- (iii) The above two limits should be connected smoothly.

Here, the local rates can be calculated based on the theory of weak interactions (see Sec. 4.3 for the local rates adopted in this paper) and the diffusion rates can be determined based on the diffusion theory (see Sec. 4.4 for the definition of the diffusion rate adopted in this paper). There will be several prescriptions to satisfy the requirement (iii) [37, 35]. In this paper, the leakage rates are defined as

$$Q_\nu^{\text{leak}} = (1 - e^{-b\tau_\nu})Q_\nu^{\text{diff}} + e^{-b\tau_\nu}Q_\nu^{\text{local}}, \quad (37)$$

$$\gamma_\nu^{\text{leak}} = (1 - e^{-b\tau_\nu})\gamma_\nu^{\text{diff}} + e^{-b\tau_\nu}\gamma_\nu^{\text{local}}, \quad (38)$$

where τ_ν is the optical depth of neutrinos and b is a parameter which is typically set as $b^{-1} = 2/3$. The optical depth can be computed from the cross sections in a standard manner [37, 35].

3.4. Explicit forms of basic equations in leakage scheme

The basic equations for the general relativistic hydrodynamics are the continuity equation, the lepton-number conservation equations, and the local conservation equation of the energy-momentum. The explicit forms of the equations are presented in this subsection for the purpose of convenience.

3.4.1. The Continuity and lepton-number conservation equations The continuity equation is

$$\nabla_\alpha(\rho u^\alpha) = 0. \quad (39)$$

As fundamental variables for numerical simulations, the following quantities are introduced: $\rho_* \equiv \rho w e^{6\phi}$ and $v^i \equiv \frac{u^i}{u^t}$ where $w \equiv \alpha u^t$. Then, the continuity equation is written as

$$\partial_t(\rho_* \sqrt{\eta}) + \partial_k(\rho_* v^k \sqrt{\eta}) = 0, \quad (40)$$

where $\sqrt{\eta} \equiv \sqrt{\det \eta_{ij}}$ is the volume element of the flat space in the curvilinear coordinates.

The lepton-number conservation equations (25) – (28) can be abbreviated as

$$\frac{dY_L}{dt} = \gamma_L, \quad (41)$$

Using the continuity equation, they become

$$\partial_t(\rho_* Y_L \sqrt{\eta}) + \partial_k(\rho_* Y_L v^k \sqrt{\eta}) = \rho_* \gamma_L. \quad (42)$$

3.4.2. *Energy-momentum conservation* As discussed in Sec. 3.1, I solve the following equations.

$$\nabla_\beta T_\alpha^\beta = -Q_\alpha^{\text{leak}}, \quad (43)$$

$$\nabla_\beta (T^{\nu,S})_\alpha^\beta = Q_\alpha^{\text{leak}}, \quad (44)$$

where $T_{\alpha\beta}$ and $(T^{\nu,S})_{\alpha\beta}$ are given by Eqs. (21) and (24), respectively. The source term Q_α^{leak} is defined by Eq. (37).

As fundamental variables for numerical simulations, I define the quantities $\hat{u}_i \equiv hu_i$ and $\hat{e} \equiv hw - P(\rho w)^{-1}$. Then, the Euler equation ($\gamma_i^\alpha \nabla_\beta T_\alpha^\beta = \gamma_i^\alpha Q_\alpha$), and the energy equation ($n^\alpha \nabla_\beta T_\alpha^\beta = n^\alpha Q_\alpha$) can be written as

$$\begin{aligned} & \partial_t (\rho_* \hat{u}_A \sqrt{\eta}) + \partial_k \left[\left\{ \rho_* \hat{u}_A v^k + P \alpha e^{6\phi} \delta_A^k \right\} \sqrt{\eta} \right] \\ &= -\rho_* \left[wh \partial_A \alpha - \hat{u}_i \partial_A \beta^i + \frac{\alpha e^{-4\phi}}{2wh} \hat{u}_k \hat{u}_l \partial_A \tilde{\gamma}^{kl} - \frac{2\alpha h(w^2 - 1)}{w} \partial_A \phi \right] \\ &+ P \partial_A (\alpha e^{6\phi}) + \frac{P \alpha e^{6\phi} \delta_A^\varpi}{\varpi} + \alpha e^{6\phi} Q_A, \end{aligned} \quad (45)$$

$$\partial_t (\rho_* \hat{u}_\varphi \sqrt{\eta}) + \partial_k (\rho_* \hat{u}_\varphi v^k \sqrt{\eta}) = \alpha e^{6\phi} Q_\varphi, \quad (46)$$

$$\begin{aligned} & \partial_t (\rho_* \hat{e} \sqrt{\eta}) + \partial_k \left[\left\{ \rho_* v^k \hat{e} + P e^{6\phi} \sqrt{\eta} (v^k + \beta^k) \right\} \sqrt{\eta} \right] \\ &= \alpha e^{6\phi} \sqrt{\eta} P K + \frac{\rho_*}{u^t h} \hat{u}_k \hat{u}_l K^{kl} - \rho_* \hat{u}_i \gamma^{ij} D_j \alpha + \alpha e^{6\phi} Q_\alpha n^\alpha, \end{aligned} \quad (47)$$

where the subscript A denotes ϖ or z component.

The evolution equations of streaming-neutrinos (E and F_i) are written as

$$\partial_t (\sqrt{\gamma} E) + \partial_k [\sqrt{\gamma} (\alpha F^k - \beta^k E)] = \sqrt{\gamma} (\alpha P^{kl} K_{kl} - F^k \partial_k \alpha + \alpha Q_a^{\text{leak}} n^a), \quad (48)$$

$$\begin{aligned} & \partial_t (\sqrt{\gamma} F_i) + \partial_k [\sqrt{\gamma} (\alpha F_i^k - \beta^k F_i)] \\ &= \sqrt{\gamma} \left(-E \partial_i \alpha + F_k \partial_i \beta^k + \frac{\alpha}{2} P^{kl} \partial_i \gamma_{kl} + \alpha Q_i^{\text{leak}} \right). \end{aligned} \quad (49)$$

3.5. Recover of primitive variables

In each numerical timestep, the so-called primitive variables (ρ , Y_L , T , and v_i) and the Lorentz factor $w = \alpha u^t = \sqrt{1 + \gamma^{ij} u_i u_j}$ must be calculated from the conserved quantities (ρ_* , $\rho_* Y_L$, \hat{e} , and \hat{u}_i), where Y_L is the representative of the lepton fractions. Since the equation of state (EOS) of the nuclear matter are usually tabularized in terms of the argument quantities (ρ , $Y_p (= Y_e)$, T), I am devoted to the cases of the tabularized EOS in the following.

In the case where the whole of the lepton-number conservation equations are solved (see Sec. 3.2), the argument quantities (ρ , Y_e , T) are calculated from the conserved quantities as follows.

- (i) Give a trial value, \tilde{w} , of the Lorentz factor. Then, one obtains a trial value, $\tilde{\rho}$, of the rest mass density: $\tilde{\rho} = \rho_* / (\tilde{w} e^{6\phi})$.
- (ii) A trial value, \tilde{T} , of the temperature can be obtained by solving

$$\hat{e} = \hat{e}_{\text{EOS}}(\tilde{\rho}, Y_e, \tilde{T}, Y_{\nu e}, Y_{\bar{\nu} e}, Y_{\nu x}), \quad (50)$$

where \hat{e}_{EOS} is constructed from EOS table. Note that \hat{e} and \hat{e}_{EOS} in general contain contributions from trapped-neutrinos. One dimensional search over the EOS table is required to obtain \tilde{T} .

- (iii) The next trial value of the Lorentz factor is given by solving $\tilde{w} = \sqrt{1 + e^{-4\phi}\tilde{\gamma}^{ij}\hat{u}_i\hat{u}_j\tilde{h}^{-2}}$, where the specific enthalpy \tilde{h} is calculated from EOS table as $\tilde{h} = \tilde{h}(\tilde{\rho}, Y_e, \tilde{T})$.
- (iv) Repeat the procedures (i)–(iii) until a required degree of convergence is achieved. Convergent solutions of the temperature and w are obtained typically within 10 iterations.

On the other hand, in the case where the total lepton fraction is evolved, the argument quantities (ρ, Y_e, T) must be recovered from the conserved quantities and Y_l under the assumption of the β -equilibrium. In this case, two-dimensional reconstruction

$$(Y_l, \hat{e}) \implies (Y_e, T) \quad (51)$$

would be required for a given \tilde{w} . In this case, there may be in general more than one couple of (Y_e, T) which gives the same Y_l and \hat{e} . Therefore, I adopt a different method to recover (ρ, Y_e, T) [27].

Under the assumption of the β -equilibrium, the electron fraction is related to the total lepton fraction as $Y_e = Y_e(\rho, Y_l, T)$. Using this relation, the original EOS table can be reconstructed in terms of the argument quantities of (ρ, Y_l, T) . Then, the same strategy as in the above can be adopted. Namely,

- (i) Give a trial value, \tilde{w} of w . Then, one obtains a trial value, $\tilde{\rho}$, of the rest mass density.
- (ii) A trial value, \tilde{T} , of the temperature can be obtained by solving

$$\hat{e} = \hat{e}_{\text{EOS}}(\tilde{\rho}, Y_l, \tilde{T}, Y_{\nu x}). \quad (52)$$

One dimensional search over the EOS table is required to obtain \tilde{T} .

- (iii) The next trial value of w is given by solving $\tilde{w} = \sqrt{1 + e^{-4\phi}\tilde{\gamma}^{ij}\hat{u}_i\hat{u}_j\tilde{h}^{-2}}$.
- (iv) Repeat the procedures (i)–(iii) until a required degree of convergence is achieved. The electron and electron neutrino fractions are given as $Y_e = Y_e(\rho, Y_l, T)$, $Y_{\nu e} = Y_{\nu e}(\rho, Y_l, T)$, $Y_{\bar{\nu}e} = Y_{\bar{\nu}e}(\rho, Y_l, T)$ in the new EOS table.

The construction of EOS table in terms of the argument variables of (ρ, Y_l, T) is important in the present implementation.

In the case of a simplified or analytic EOS, the Newton-Raphson method may be applied to recover the primitive variables. In the case of tabulated EOS, by contrast, the Newton-Raphson method may not good approach since it requires derivatives of thermodynamical quantities which in general cannot be calculated precisely from tabulated EOS by the finite differentiating method (see also Sec. 4.2).

4. Specific details of microphysics

4.1. Equation of state

Baryons. While any EOS table can be used in the present code, an EOS [51, 52] based on the relativistic mean field theory is adopted for baryon EOS (hereafter denoted by Shen EOS) in the present version of our code. Note that the causality is guaranteed to be satisfied in the relativistic EOS, whereas the sound velocity sometimes exceeds the velocity of the light in the non-relativistic framework, e.g., in the EOS by Lattimer and Swesty [53].

Electrons and Positrons. If a EOS table for baryons does not include the contributions of the leptons (electrons, positrons, and neutrinos if necessary) and photons, one has to consistently include these contributions to the table. Electrons and positrons are described as ideal Fermi gases.

To consistently calculate the contribution of the electrons, the charge neutrality condition $Y_p = Y_e$ should be solved in terms of the electron chemical potential μ_e , for each value of the baryon rest-mass density ρ and the temperature T in the EOS table:

$$n_e(\mu_e, T) \equiv n_- - n_+ = \frac{\rho Y_p}{m_u} \quad (53)$$

in terms of μ_e for given ρ , T , and Y_p . Here, $m_u = 931.49432$ MeV is the atomic mass unit, and n_- and n_+ are the total number densities (i.e., including electron-positron pairs) of electrons and positrons, respectively. Then all other quantities can be calculated from T and μ_e .

Radiations. The contribution of radiations is included in a standard manner: The radiation pressure and the specific internal energy density are given by

$$\varepsilon_r = \frac{a_r T^4}{\rho}, \quad P_r = \frac{a_r T^4}{3}, \quad (54)$$

where a_r is the radiation constant $a_r = (8\pi^5 k_B^4)(15c^3 h_P^3)^{-1}$ and k_B and h_P are the Boltzmann's and the Planck's constants respectively.

Trapped-Neutrinos. In this paper, the trapped-neutrinos are assumed to interact sufficiently frequently with matter that be thermalized. Therefore they are described as ideal Fermi gases with the matter temperature. Then, from the neutrino fractions Y_ν , the chemical potentials of neutrinos are calculated by solving

$$Y_\nu = Y_\nu(\mu_\nu, T). \quad (55)$$

Using the chemical potentials and the matter temperature, the pressure and the internal energy of the trapped-neutrinos are calculated.

4.2. The sound velocity

In high-resolution shock-capturing schemes, it is in general necessary to evaluate the sound velocity c_s ,

$$c_s^2 = \frac{1}{h} \left[\left. \frac{\partial P}{\partial \rho} \right|_\epsilon + \frac{P}{\rho} \left. \frac{\partial P}{\partial \epsilon} \right|_\rho \right]. \quad (56)$$

Here, the derivatives of the pressure are calculated by

$$\left. \frac{\partial P}{\partial \rho} \right|_{\epsilon} = \sum_{i=B,e,r,\nu} \left[\left. \frac{\partial P_i}{\partial \rho} \right|_T - \left. \frac{\partial P_i}{\partial T} \right|_{\rho} \left(\sum_{j=B,e,r,\nu} \left. \frac{\partial \epsilon_j}{\partial \rho} \right|_T \right) \left(\sum_{k=B,e,r,\nu} \left. \frac{\partial \epsilon_k}{\partial T} \right|_{\rho} \right)^{-1} \right] \quad (57)$$

$$\left. \frac{\partial P}{\partial \epsilon} \right|_{\rho} = \left(\sum_{i=B,e,r,\nu} \left. \frac{\partial P_i}{\partial T} \right|_{\rho} \right) \left(\sum_{j=B,e,r,\nu} \left. \frac{\partial \epsilon_j}{\partial T} \right|_{\rho} \right)^{-1}, \quad (58)$$

where 'B', 'e', 'r', and ν in the sum denote contributions of the baryon, the electrons, radiations, and neutrinos, respectively.

Since there are in general the phase transition regions in a EOS table for baryons and the EOS moreover may contain some non-smooth spiky structures, careful treatments are necessary when evaluating the derivatives of thermodynamical quantities. In the present EOS table, the derivatives are carefully evaluated so that there are no spiky behaviors in the resulting sound velocities.

4.3. The local rates

In this paper, the electron and positron captures (γ_{ν}^{ec} and γ_{ν}^{pc}) [54], the electron-positron pair annihilation ($\gamma_{\nu}^{\text{pair}}$) [55], the plasmon decays ($\gamma_{\nu}^{\text{plas}}$) [37], and the Bremsstrahlung processes ($\gamma_{\nu}^{\text{Brems}}$) [56] are considered as the local production reactions of neutrinos. Then, the local rates for lepton fractions are

$$\gamma_e^{\text{local}} = \gamma_{\nu}^{\text{ec}} - \gamma_{\nu}^{\text{pc}}, \quad (59)$$

$$\gamma_{\nu e}^{\text{local}} = \gamma_{\nu}^{\text{ec}} + \gamma_{\nu}^{\text{pair}} + \gamma_{\nu}^{\text{plas}} + \gamma_{\nu}^{\text{Brems}}, \quad (60)$$

$$\gamma_{\nu e}^{\text{local}} = \gamma_{\nu}^{\text{pc}} + \gamma_{\nu}^{\text{pair}} + \gamma_{\nu}^{\text{plas}} + \gamma_{\nu}^{\text{Brems}}, \quad (61)$$

$$\gamma_{\nu x}^{\text{local}} = \gamma_{\nu}^{\text{pair}} + \gamma_{\nu}^{\text{plas}} + \gamma_{\nu}^{\text{Brems}}. \quad (62)$$

Similarly, the local energy emission rate Q_{ν}^{local} is the sum of the contributions of the electron and positron captures (Q_{ν}^{ec} and Q_{ν}^{pc}), the electron-positron pair annihilation (Q_{ν}^{pair}), the plasmon decays (Q_{ν}^{plas}), and Bremsstrahlung processes (Q_{ν}^{Brems}).

4.4. The diffusion rates

I follow [35] for the neutrino diffusion rates $\gamma_{\nu}^{\text{diff}}$ and Q_{ν}^{diff} . I present the forms of the diffusion rates in the following for convenience. An alternative definition of the diffusion rates will be found in [37]. The cross sections adopted in this paper are those of neutrino-nucleus and neutrino-nucleon scattering, and neutrino absorptions on free nucleons. Explicit forms of these cross sections will be found in [56]

Ignoring the higher order corrections, the neutrino cross sections can be written in general as

$$\sigma(E_{\nu}) = E_{\nu}^2 \tilde{\sigma}, \quad (63)$$

where E_{ν} is the neutrino energy and $\tilde{\sigma}$ is 'cross section' in which E_{ν}^2 dependence is factored out. Similarly, the opacity and the optical depth are written as

$$\kappa(E_{\nu}) = \sum \kappa_i(E_{\nu}) = E_{\nu}^2 \sum \tilde{\kappa}_i = E_{\nu}^2 \tilde{\kappa}, \quad (64)$$

$$\tau(E_\nu) = \int \kappa(E_\nu) ds = E_\nu^2 \int \tilde{\kappa} ds = E_\nu^2 \tilde{\tau}. \quad (65)$$

Now the neutrino diffusion time may be defined by [37, 35]

$$T_\nu^{\text{diff}}(E_\nu) \equiv \frac{\Delta x(E_\nu)}{c} \tau(E_\nu) = E_\nu^2 a^{\text{diff}} \frac{\tilde{\tau}^2}{c\tilde{\kappa}} = E_\nu^2 \tilde{T}_\nu^{\text{diff}}, \quad (66)$$

where the distance parameter $\Delta x(E_\nu)$ is set to be

$$\Delta x(E_\nu) = a^{\text{diff}} \frac{\tau(E_\nu)}{\kappa(E_\nu)}. \quad (67)$$

Here a_{diff} is a parameter which controls the diffusion rates. In this paper, I adopt $a_{\text{diff}} = 3$ as suggested in [37].

Finally, the neutrino diffusion rates are defined as

$$N_\nu^{\text{diff}} \equiv \int \frac{n_\nu(E_\nu)}{T_\nu^{\text{diff}}(E_\nu)} dE_\nu = \frac{1}{a^{\text{diff}}} \frac{4\pi c g_\nu}{(h_{PC})^3} \frac{\tilde{\kappa}}{\tilde{\tau}^2} T F_0(\eta_\nu), \quad (68)$$

$$Q_\nu^{\text{diff}} \equiv \int \frac{E_\nu n_\nu(E_\nu)}{T_\nu^{\text{diff}}(E_\nu)} dE_\nu = \frac{1}{a^{\text{diff}}} \frac{4\pi c g_\nu}{(h_{PC})^3} \frac{\tilde{\kappa}}{\tilde{\tau}^2} T^2 F_1(\eta_\nu), \quad (69)$$

from which the diffusion rates Q_ν^{diff} and γ_ν^{diff} are easily calculated. Here, g_ν is the statistical weight factor for neutrinos and $n(E_\nu)dE_\nu$ is the number density of neutrino in the range from E_ν to $E_\nu + dE_\nu$ under the Fermi-Dirac distribution.

5. Validity of general relativistic leakage scheme

5.1. Brief summary of numerical set up

The numerical schemes for solving the Einstein's equations are essentially same as those in [4]; We adopt so-called BSSN formulation [58, 59] and use 4th-order finite difference scheme in the spatial direction and the 3rd-order Runge-Kutta scheme in the time integration. The advection terms such as $\beta^i \partial_i \phi$ are evaluated by a 4th-order upwind scheme. The hydrodynamic equations, the lepton-number conservation equations, and

Model		$\Phi_c \leq 0.0125$	$\leq \Phi_c \leq 0.025$	$\leq \Phi_c \leq 0.05$	$\leq \Phi_c \leq 0.1$	$\Phi_c \geq 0.1$
S15	Δx_0	3.26	1.60	0.820	0.414	0.217
	η	1.005	1.005	1.005	1.005	1.005
	N	444	668	924	1212	1532
	L (km)	2330	2239	2188	2124	2103
S15 low resolution	Δx_0	5.10	2.90	1.44	0.760	0.396
	η	1.005	1.005	1.005	1.005	1.005
	N	316	444	636	828	1020
	L (km)	2244	2151	2073	2043	

Table 1. Summary of the regridding procedure. The values of the minimum grid spacing Δx_0 (in units of km), the non-uniform-grid factor η , and the grid number N for each range of $\Phi_c = 1 - \alpha_c$ are listed.

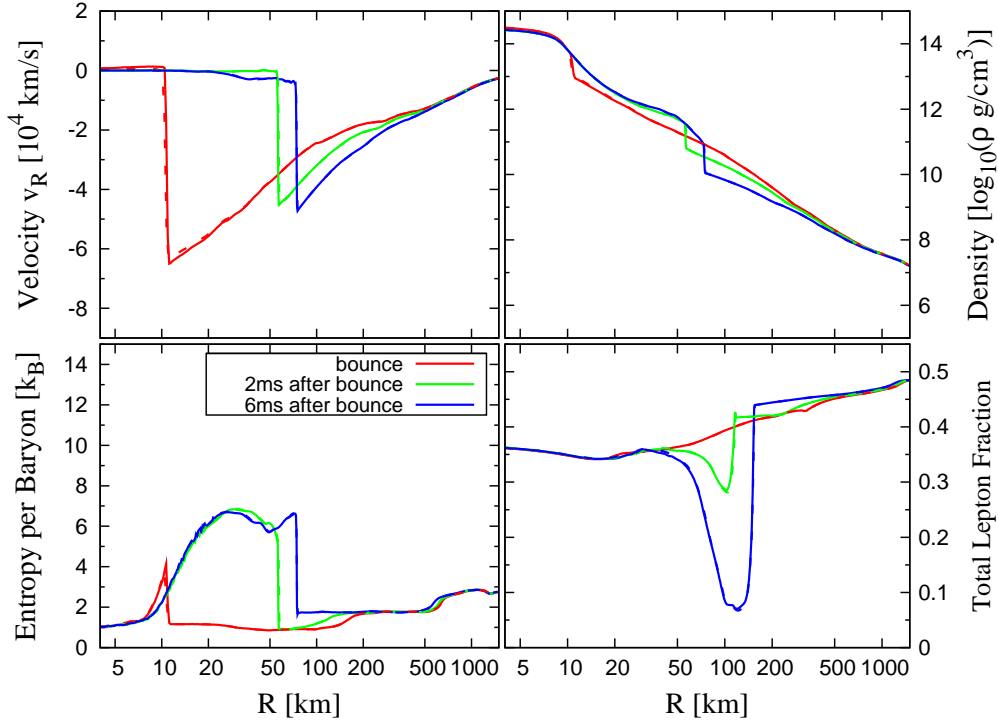


Figure 1. The radial profiles of the infall velocity, the density, the entropy per baryon and the total lepton fraction at bounce, 2 ms and 6 ms after bounce. The results for the finer grid resolution (solid curve) and for the coarser grid resolution (the dotted curves) are shown together while they are almost identical.

equations of streaming-neutrinos are solved using the high-resolution centered scheme [62].

A nonuniform grid is adopted in the numerical simulation, in which the grid spacing increases as

$$dx_{j+1} = \eta dx_j, \quad dz_{l+1} = \eta dz_l \quad (70)$$

where $dx_j \equiv x_{j+1} - x_j$, $dz_l \equiv z_{l+1} - z_l$ and η is a constant. The regridding procedure [60, 61] is furthermore used to compute the collapse accurately and to save the CPU time efficiently. For the regridding, I define an effective gravitational potential $\Phi_c \equiv 1 - \alpha_c$ ($\Phi_c > 0$) where α_c is the central value of the lapse function. In Table 1, parameters of the regridding procedure are summarized. More detailed set up of the simulation will be found elsewhere [63].

As a test problem, I performed a collapse simulation of spherical presupernova core. A presupernova model (S15) of $15M_\odot$ with solar metallicity computed in [57] is adopted as the initial condition. I follow the dynamical evolution of central part which is composed of the Fe core and some part of the Si-shell. The density, the electron fraction, and the temperature are used to calculate other thermodynamical quantities using the EOS table.

To check the validity of the code, the results are compared with those in the state-of-

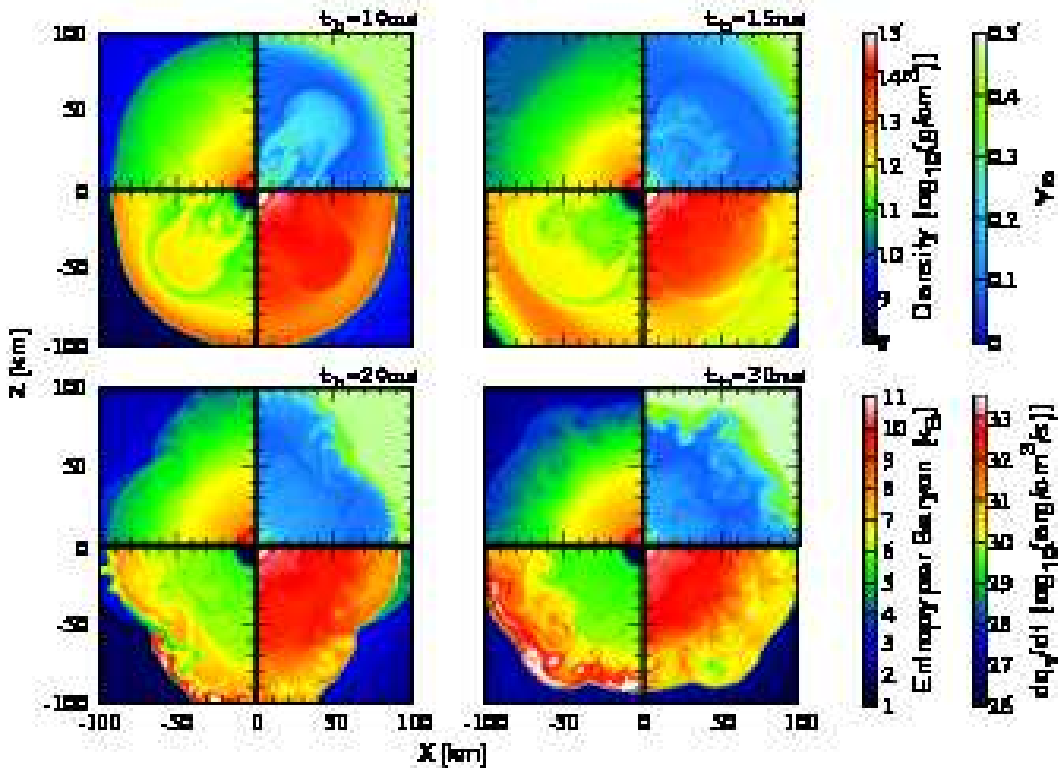


Figure 2. Snapshots of the contours of the density (top left panels), the electron fraction Y_e (top right panels), the entropy per baryon (bottom left panels), and the local neutrino energy emission rate (bottom right panels) in the x - z plane at selected time slices.

the-art one-dimensional simulations (hereafter, the reference simulations) in full general relativity [64, 21, 65, 22], where one dimensional general relativistic Boltzmann equation is solved for neutrino transfer with relevant weak interaction processes. Since neutrino heating processes ($\nu_e + n \rightarrow p + e^-$ and $\bar{\nu}_e + p \rightarrow n + e^+$) are not include in the present implementation, and multidimensional effects such as convection cannot be followed in the one-dimensional reference simulations, I pay particular attention in comparing results during the collapse and the early phase ($\sim 10 \text{ ms}$) after the bounce. After that, direct comparison cannot be done since in the present multidimensional code convective activities set in. As shown below, results in the present simulation and in the reference simulations agree well.

5.2. Comparison of the radial profiles

The collapse proceeds until the nuclear density is reached in the central part of the iron core. Then, the inner core experiences the bounce due to the nuclear repulsive forces, forming a strong shock wave at the edge of the inner core. The shock wave propagates outward and when it crosses the neutrino-sphere, spiky burst emissions of neutrinos occur (neutrino bursts): Neutrinos in hot post-shock region are copiously

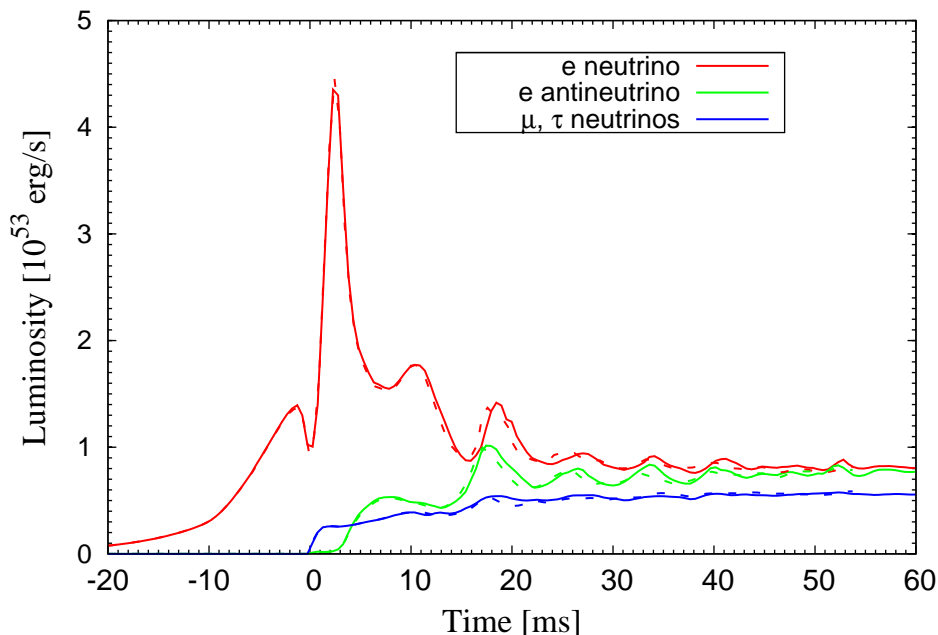


Figure 3. Time evolution of the neutrino luminosities. The results in the finer grid resolution (solid curves) and in the coarser grid resolution (dashed curves) are shown together. The two results are almost identical until the convective phase sets in, while they are not in the convective phase.

emitted without interacting matters. Eventually, negative gradients of the total lepton fraction are formed behind the shock since neutrinos carry away the lepton number. In Fig. 1, we show the radial profiles of the infall velocity, the density, the entropy per baryon and the total lepton fraction at selected time slices.

The results agree at least semi-quantitatively with those in [64, 21, 65, 22]. In particular, the radial profiles of the infall velocity, the density, and the entropy per baryon show good agreements. No such good agreements was reported in the previous Newtonian simulations in which leakage schemes are adopted [28, 29, 31, 32, 30]. The negative gradients quantitatively are little bit steeper in the present simulation. The reason may be partly because the *transfers* of lepton-number and energy are not solved in the present leakage scheme. Except for this quantitative difference, the two results agree well. It is found that the difference can be reduced by adjusting the parameter a_{diff} introduced in Sec. 4.4.

Recall that regions of negative Y_l gradient are known to be convectively unstable [36]. Convective activities indeed set in in the present simulation as shown in Fig. 2.

5.3. Comparison of the Neutrino luminosities

Comparisons of the neutrino luminosities are particularly important since they depend on both implementations of weak interactions (especially electron capture in the present

case) and treatments of neutrino cooling (the detailed leakage scheme). Also, accurate estimations of neutrino luminosities would be primarily important for astrophysical applications, since neutrinos carry away the most of energy liberated during the collapse as the main cooling source.

In Fig. 3, I show neutrino luminosities calculated according to [50]

$$L_\nu = \int \alpha e^{6\phi} u_t \dot{Q}_\nu^{\text{leak}} d^3x, \quad (71)$$

as functions of $t - t_{\text{bounce}}$ where t_{bounce} is time at the bounce. The result also agrees approximately with that in the reference simulations. The neutrino bursts occur when the shock wave crosses the neutrino-sphere soon after the bounce. The peak luminosity at the neutrino burst is $L_{\nu_e} \approx 4.5 \times 10^{53}$ ergs/s in the present simulation, which agrees well with that in the reference simulations. The peak luminosity and the duration (width) of the neutrino burst emission can be improved by adjusting the parameter a_{diff} . The modulation found in the later phase $t - t_{\text{bounce}} > 10$ ms is due to convective activities driven by negative gradients of electron fraction and entropy per baryon.

Thus, Fig. 3 illustrates that the present detailed leakage scheme works fairly well and may be applied to simulations of rotating core collapse to a black hole and mergers of binary neutron stars.

In the previous simulations based on the leakage scheme [32, 27] where the single 'neutrino-trapping' density is adopted, the luminosities do not agree with that in the reference simulations. In particular, the luminosities at the neutrino bursts are quite different.

5.4. Convergence

In Figs. 1 and 3, I show results in the higher resolution (solid curves) and the lower resolution (dashed curves). The radial profiles of the two resolutions are almost identical, showing that convergent results are obtained in the present simulation (see Fig. 1). In the time evolution of neutrino luminosities (see Fig. 3), the two results are almost identical before the convective activities set in. In the later phase, on the other hand, the two results shows slight difference. Since the convection and the turbulence can occurs in a infinitesimal scale length, the smaller-scale convection and turbulence are captured in the finer grid resolution. Further discussions associated with the convergence and numerical accuracy will be found in [63].

6. Summary and Discussions

6.1. Summary

In this paper, I presented an implementation of the weak interactions and the neutrino cooling in the framework of full general relativity. Since the characteristic timescale of weak interaction processes $t_{\text{wp}} \sim |Y_e/\dot{Y}_e|$ is much shorter than the dynamical timescale t_{dyn} in hot dense matters, stiff source terms appears in the equations. In general, an

implicit scheme may be required to solve them [40]. However, it is not clear whether implicit schemes do work or not in the relativistic framework. The Lorentz factor is coupled with the rest mass density and the energy density. The specific enthalpy is also coupled with the momentum. Due to these couplings, it is very complicated to recover the primitive variables and the Lorentz factor from conserved quantities. Therefore I proposed an explicit method to solve the equations noting that the characteristic timescale of neutrino leakage from the system t_{leak} is much longer than t_{wp} and is comparable to t_{dyn} .

By decomposing the energy tensor of neutrino into the trapped-neutrino and the streaming-neutrino parts, the equations for the energy momentum tensor can be rewritten so that the source terms are characterized by the leakage timescale t_{leak} (see Eqs. (20) and (17)). The lepton-number conservation equations, on the other hand, include the source terms characterized by the WP timescale. Therefore the *limiters* for the stiff source terms are introduced to solve the lepton-number conservation equations explicitly (see Sec. 3.2).

In the numerical relativistic hydrodynamics, it is required to calculate the primitive variables and the Lorentz factor from the conserved quantities. In this paper, I develop a robust and stable procedure for it (Sec. 3.5).

Finally, to check the validity of the present implementation, I performed a collapse simulation of spherical presupernova core and compared the results with those obtained in the state-of-the-art one-dimensional simulations in full general relativity [64, 21, 65, 22]. As shown in this paper, results in this paper agree well with those in the state-of-the-art simulations. Thus the present implementation will be applied to simulations of rotating core collapse to a black hole and mergers of binary neutron stars.

6.2. Discussions

Since the present implementation of the microphysics is simple and explicit, it has advantage that the individual microphysical processes can be easily improved and sophisticated.

For example, the neutrino emission via the electron capture can be easily sophisticated as follows. To precisely calculate the electron capture rate, the complete information of the parent and daughter nuclei are required. In the nuclear equations of state currently available, however, a representative single-nucleus average for the true ensemble of heavy nuclei is adopted. The representative is usually the most abundant nuclei. The problem in evaluating the capture rate is that the nuclei which cause the largest changes in Y_e are neither the most abundant nuclei nor the nuclei with the largest rates, but the combination of the two. In fact, the most abundant nuclei tend to have small rates since they are more stable than others, and the fraction of the most reactive nuclei tend to be small [66, 67]. Assuming that the nuclear statistical equilibrium (NSE) is achieved, the electron capture rates under the NSE ensemble of heavy nuclei may be calculated for given (ρ, Y_e, T) . Such a numerical rate table can be easily employed in

the present implementation.

Also, the neutrino cross sections can be improved. As summarized in [68], there are a lot of higher order corrections to the neutrino opacities. Note that small changes in the opacities may result in much larger changes in the neutrino luminosities, since the neutrino energy emission rates strongly depend on the temperature and the temperature at the last scattering surface ($\tau_\nu \sim \sigma T^2 \sim 1$) changes as $T \sim \sigma^{-1/2}$. Although the correction terms are in general very complicated, it is straightforward to include the corrections in the present implementation. Note that the corrections become more important for higher neutrino energies. Therefore, the correction terms might play roles in the collapse of population III stellar core and the formation of a black hole in which very high temperatures ($T > 100$ MeV) are achieved. I already started studies to explore the importance of these corrections in the case of black hole formation.

As briefly described in the introduction, one of main drawbacks of the present implementation of the neutrino cooling is that the *transfer* of neutrinos are not solved. Although to *fully* solve the transfer equations of neutrinos is far beyond the scope of this paper, there are a lot of rooms for improvements in the treatment of the neutrino cooling. For example, the relativistic moment formalism [69, 70], in particular the so-called M1 closure formalism, may be adopted. For this purpose, a more sophisticated treatment of the closure relation for $P_{\alpha\beta}$ is required. For example, one may adopt the Eddington tensor of the form [71]

$$P_{\alpha\beta} = \left[\frac{1-\chi}{2} \gamma_{\alpha\beta} + \frac{3\chi-1}{2} \frac{F_\alpha F_\beta}{F_\gamma F_\gamma} \right] E, \quad (72)$$

where χ is the (variable) Eddington factor. In the diffusion limit where the neutrino pressure is isotropic $\chi = 1/3$, while in the free streaming limit $\chi = 1$. We plan to implement a relativistic M1 closure formalism for the neutrino transfer in the near future.

To conclude, the present implementation of microphysics in full general relativity works fairly well. We are now in the standpoint where simulations of stellar core collapse to a black hole and merger of compact stellar binaries can be performed including microphysical processes. Fruitful scientific results will be reported in the near future.

acknowledgments

I thank M. Shibata and L. Rezzolla for valuable discussions, and the referees for valuable comments. I also thank T. Shiromizu and T. Fukushima for their grateful aids. Numerical computations were performed on the NEC SX-9 at the data analysis center of NAOJ and on the NEC SX-8 at YITP in Kyoto University. This work is partly supported by the Grant-in-Aid of the Japanese Ministry of Education, Science, Culture, and Sport (21018008, 21105511).

References

- [1] van Riper K A 1988 *Astrophys. J.* **329** 339
- [2] Takahara M and Sato K 1984 *Prog. Theor. Phys.* **72** 978
- [3] Ott C D 2009 *Class. Quant. Grav.* **26** 063001
- [4] Kiuchi K et al. 2009 *Phys. Rev. D* **80** 064037
- [5] Faber J 2009 *Class. Quant. Grav.* **26** 1104004
- [6] Kulkarni S R et al. 1998 *Nature* **395** 663
- [7] Galama T J et al. 1998 *Nature* **395** 670
- [8] Hjorth J et al. 2003 *Nature* **423** 847
- [9] Stanek K Z et al. 2003 *Astrophys. J.* **591** L17
- [10] Kawabata K S et al. 2003 *Astrophys. J.* **593** L19
- [11] Modjaz M et al. 2006 *Astrophys. J.* **645** L21
- [12] Sollerman J et al. 2006 *Astron. Astrophys.* **454** 503
- [13] Nakar E 2007 *Phys. Rep.* **442** 166
- [14] Lee W H and Ramirez-Ruiz E 2007 *New J. Phys.* **9** 17
- [15] Abramovici A et al. 1992 *Science* **256** 325
- [16] Acernese F et al. 2004 *Class. Quant. Grav.* **21** S385
- [17] Willke B et al. 2002 *Class. Quant. Grav.* **19** 1377
- [18] Dimmelmeier H et al. 2002 *Astron. Astrophys.* **393** 523
- [19] Shibata M and Sekiguchi Y 2003 *Phys. Rev. D* **68** 104020
- [20] Yamada S Janka H Th and Suzuki H 1999 *Astron. Astrophys.* **344** 533
- [21] Liebendörfer M et al. 2004 *Astrophys. J. Suppl.* **150** 263
- [22] Sumisyoishi K et al. 2005 *Astrophys. J.* **629** 922
- [23] Mezzacappa A and Matzner R 1989 *Astrophys. J.* **343** 853
- [24] Ott C D et al. 2007 *Phys. Rev. Lett.* **98** 261101
- [25] Dimmelmeier H et al. 2007 *Phys. Rev. Lett.* **98** 251101
- [26] Liebendörfer M 2005 *Astrophys. J.* **633** 1042
- [27] Sekiguchi Y 2007 *PhD thesis* (University of Tokyo)
- [28] Epstein R I and Pethick C J 1981 *Astrophys. J.* **243** 1003
- [29] van Riper K A and Lattimer J M 1981 *Astrophys. J.* **249** 270
- [30] Baron E A, Cooperstein J, and Kahana S 1985 *Nucl. Phys. A* **440** 744
- [31] Cooperstein J 1988 *Phys. Rep.* **163** 95
- [32] Kotake K et al. 2003 *Astrophys. J.* **595** 304
- [33] Ott et al. 2008 *Astrophys. J.* **685** 1069
- [34] Bethe H A and Wilson J R 1985 *Astrophys. J.* **295** 14
- [35] Rosswog S and Liebendörfer M 2003 *Mon. Not. R. Astron. Soc.* **342** 673
- [36] Bethe H A 1990 *Rev. Mod. Phys.* **62** 801
- [37] Ruffert R et al. 1996 *Astron. Astrophys.* **311** 532
- [38] Liebendörfer M Whitehouse S C and Fischer T 2009 *Astrophys. J.* **698** 1174
- [39] Bowers R L and Wilson J R 1982 *Astrophys. J. Suppl.* **50** 115
- [40] Bruenn S W 1985 *Astrophys. J. Suppl.* **58** 771
- [41] Myra E et al. 1987 *Astrophys. J.* **318** 744
- [42] Mezzacappa A and Bruenn S W 1993 *Astrophys. J.* **405** 669
- [43] Rampp M. and Janka H -Th 2002 *Astron. Astrophys.* **396** 361
- [44] Livne E et al. 2004 *Astrophys. J.* **609** 277
- [45] Buras R et al. 2006 *Astron. Astrophys.* **447** 1049
- [46] Burrows A et al. 2007 *Astrophys. J.* **655** 416
- [47] Marek A and Janka H Th 2009 *Astrophys. J.* **694** 664
- [48] Mezzacappa A and Messer O E B 1999 *J. Comp. Appl. Math.* **109** 281
- [49] Misner C W and Sharp D H 1964 *Phys. Rev.* **136** B571

- [50] Shibata M Sekiguchi Y and Takahashi R 2007 *Prog. Theor. Phys.* **118** 257
- [51] Shen H et al. 1998 *Nucl. Phys. A* **637** 435
- [52] Shen H et al. 1998 *Prog. Theor. Phys.* **100** 1013
- [53] Lattimer J M and Swesty F D 1991 *Nucl. Phys. A* **535** 331
- [54] Fuller G M et al. 1985 *Astrophys. J.* **293** 1
- [55] Cooperstein J et al. 1986 *Astrophys. J.* **309** 653
- [56] Burrows A et al. 2006 *Nucl. Phys. A* **777** 356
- [57] Woosley S E et al. 2002 *Rev. Mod. Phys.* **74** 1015
- [58] Shibata M and Nakamura T 1995 *Phys. Rev. D* **52** 5428
- [59] Baumgarte T W and Shapiro S L 1999 *Phys. Rev. D* **59** 024007
- [60] Shibata M and Shapiro S L 2002 *Astrophys. J.* **572** L39
- [61] Sekiguchi Y and Shibata M 2005 *Phys. Rev. D* **71** 084013
- [62] Kruganov A and Tadmor E 2000 *J. Comput. Phys.* **160** 241
- [63] Sekiguchi Y 2010 *Prog. Theor. Phys.* submitted
- [64] Liebendörfer M et al. 2001 *Phys. Rev. D* **63** 103004
- [65] Liebendörfer M et al. 2005 *Astrophys. J.* **620** 840
- [66] Aufderheide M B et al. 1994 *Astrophys. J. Suppl.* **91** 389
- [67] Janka H -Th et al. 2007 *Phys. Rept.* **442** 38
- [68] Horowitz C J 2002 *Phys. Rev. D* **65** 043001
- [69] Anderson J L and Spiegel E A 1972 *Astrophys. J.* **171** 127
- [70] Thorne K S 1981 *Mon. Not. R. Astron. Soc.* **194** 439
- [71] Levermore C D and Pomraning G C 2005 *Astrophys. J.* **248** 321